Tunable light absorption of Si nanowires by coating non-absorbing dielectric shells for photovoltaic applications

WENFU LIU
Department of Electronic Science and Engineering, Huanghuai University, Zhumadian, Henan 463000, China

We present a detailed analysis of the light absorption in the coaxial nanowire (NW) of Si core and nonabsorbing dielectric shell which has great potential in solar cells. We have calculated the absorption efficiency within the framework of the Lorenz-Mie light scattering theory to investigate the effects of the core radius, the shell thickness, and the shell refractive index on the light absorption. We have found that the photocurrent can be enhanced up to ~135% for the coaxial NW of the core radius of 150 nm by tuning the shell thickness and the shell refractive index, as compared to Si NW.

1. Introduction

Si nanowires (NWs) have received great attention due to their excellent optical/ electrical properties and potentials in optoelectronic applications, especially in photovoltaic (PV) areas [1-5]. It has been demonstrated that the light absorption in semiconductor NWs can be enhanced by tuning the radius due to the excitation of the leaky mode resonances (LMRs) [6,7]. Recently, we have also reported that the light absorption in single NWs can be further enhanced by coating the non-absorbing dielectric shells [8,9]. However, there is still a lack of analytical investigation of the light absorption in such coaxial NWs.

In this paper, we further report the effects of the shell thickness and the shell refractive index on the light absorption in the coaxial NWs for four representative Si core radii. We have found out that the absorption efficiency strongly depends on the shell thickness and the shell refractive index at a fixed core radius. As a result, we have obtained ~135% increase of the photocurrent.

2. Theory background

A schematic of the cross section of coaxial NWs comprised of Si cores and nonabsorbing dielectric shells is shown in Fig. 1. The coaxial NWs can be characterized by the Si core radius r, the total radius R, and the nonabsorbing shell thickness t (i.e. $t = R - r$).
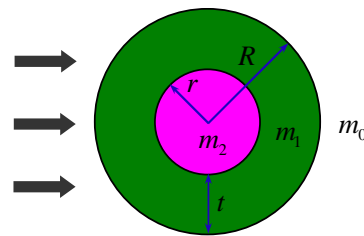
Fig. 1. A schematic of the cross section of the coaxial NW. r and R are radii of the Si core and dielectric shell, respectively. Corresponding refractive indices, m_0 (air), m_1 (shell), and m_2 (core) are indicated. Thick arrows denote the incident light. t is the shell thickness.

We have calculated the light absorption of such coaxial NWs in the framework of Lorenz-Mie light scattering theory [10], where NWs are treated as infinitely long cylinders, which has been well-applied to describing the light absorption of various single NWs [6-9,11]. We have employed the perpendicular incident light with an incident propagation vector $\boldsymbol{k_0}$ to the NW axis as indicated by thick arrows in the figure, the wavelength range of 310 to 1127 nm covering the major solar spectrum (AM 1.5G), the complex refractive index of Si (m_2) taken from Ref. [12], and the refractive index of the shell (m_1) that is real and kept constant under our investigation. By solving Maxwell's equations with the boundary conditions at the core/shell and shell/air interfaces [8-10], we can obtain the absorption efficiencies of extinction Q_{ext}, scattering Q_{sca} and absorption Q_{abs}, defined as the ratio of the corresponding cross sections to the geometrical cross section of NWs [10]:

$$Q_{ext}^{TM} = \frac{2}{x}\mathrm{Re}\left\{\sum_{n=-\infty}^{\infty} b_n\right\}, \ Q_{ext}^{TE} = \frac{2}{x}\mathrm{Re}\left\{\sum_{n=-\infty}^{\infty} a_n\right\}, \quad (1a)$$

$$Q_{sca}^{TM} = \frac{2}{x}\left\{\sum_{n=-\infty}^{\infty} |b_n|^2\right\}, \ Q_{sca}^{TE} = \frac{2}{x}\left\{\sum_{n=-\infty}^{\infty} |a_n|^2\right\}, \quad (1b)$$

$$Q_{abs}^{TM} = Q_{ext}^{TM} - Q_{sca}^{TM}, \ Q_{abs}^{TE} = Q_{ext}^{TE} - Q_{sca}^{TE}, \qquad (1c)$$

where the superscripts TM and TE represent the transverse-magnetic (electric field parallel to the axis) and transverse-electric (electric field perpendicular to the axis) illuminations, respectively. $x = k_0 r$. Note here that r but not R is used since we assume that the shells have no contribution to the light absorption. a_n and b_n are far-field scattering coefficients:

$$a_n = a_{n0} / \Delta_n^{TE}, \ b_n = b_{n0} / \Delta_n^{TM}. \qquad (2)$$

with

$$b_{n0} = \begin{vmatrix} 0 & J_n(m_1 k_0 r) & H_n(m_1 k_0 r) & -J_n(m_2 k_0 r) \\ 0 & m_1 J_n'(m_1 k_0 r) & m_1 H_n'(m_1 k_0 r) & -m_2 J_n'(m_2 k_0 r) \\ J_n(m_0 k_0 R) & J_n(m_1 k_0 R) & H_n(m_1 k_0 R) & 0 \\ m_0 J_n'(m_0 k_0 R) & m_1 J_n'(m_1 k_0 R) & m_1 H_n'(m_1 k_0 R) & 0 \end{vmatrix}, \quad (3a)$$

$$\Delta_n^{TM} = \begin{vmatrix} 0 & J_n(m_1 k_0 r) & H_n(m_1 k_0 r) & -J_n(m_2 k_0 r) \\ 0 & m_1 J_n'(m_1 k_0 r) & m_1 H_n'(m_1 k_0 r) & -m_2 J_n'(m_2 k_0 r) \\ H_n(m_0 k_0 R) & J_n(m_1 k_0 R) & H_n(m_1 k_0 R) & 0 \\ m_0 H_n'(m_0 k_0 R) & m_1 J_n'(m_1 k_0 R) & m_1 H_n'(m_1 k_0 R) & 0 \end{vmatrix}, \quad (3b)$$

$$a_{n0} = \begin{vmatrix} 0 & J_n'(m_1 k_0 r) & H_n'(m_1 k_0 r) & -J_n'(m_2 k_0 r) \\ 0 & m_1 J_n(m_1 k_0 r) & m_1 H_n(m_1 k_0 r) & -m_2 J_n(m_2 k_0 r) \\ J_n'(m_0 k_0 R) & J_n'(m_1 k_0 R) & H_n'(m_1 k_0 R) & 0 \\ m_0 J_n(m_0 k_0 R) & m_1 J_n(m_1 k_0 R) & m_1 H_n(m_1 k_0 R) & 0 \end{vmatrix}, \quad (3c)$$

$$\Delta_n^{TE} = \begin{vmatrix} 0 & J_n'(m_1 k_0 r) & H_n'(m_1 k_0 r) & -J_n'(m_2 k_0 r) \\ 0 & m_1 J_n(m_1 k_0 r) & m_1 H_n(m_1 k_0 r) & -m_2 J_n(m_2 k_0 r) \\ H_n'(m_0 k_0 R) & J_n'(m_1 k_0 R) & H_n'(m_1 k_0 R) & 0 \\ m_0 H_n(m_0 k_0 R) & m_1 J_n(m_1 k_0 R) & m_1 H_n(m_1 k_0 R) & 0 \end{vmatrix}, \quad (3d)$$

where $J_n()$ and $H_n()$ are Bessel and Hankel functions of the first kind, respectively. The prime superscript (′) denotes the derivative with respect to the argument r or R.

For non-polarized incident light like sunlight,

$$Q_{abs} = (Q_{abs}^{TM} + Q_{abs}^{TE})/2. \qquad (4)$$

The absorption efficiency Q_{abs} has then been calculated to examine the light absorption capability of the coaxial NWs.

3. Results and discussion

3.1 Single Si NWs

If $m_1 = m_0 = 1$, Eqs. (1)-(4) represent the case of single Si NWs. In Fig. 2(a-b), we show two-dimensional (2D) color maps of the absorption efficiency Q_{abs} as a function of the illumination wavelength λ and NW radius r for TM- and TE-polarized illuminations, respectively. These maps provide an insight into the absorption behavior of NWs due to the resonant modes and their polarization dependence. Note here that the peaks in the absorption spectra can be identified with the excitation of specific LMRs of the cylindrical structures. The modes can be expressed as TM_{ml} and TE_{ml}, where m and l are the

azimuthal mode number and the radial order of the resonances, respectively. The location of each absorption peak can be labeled in terms of the LMRs as shown in the figures. One can see that the absorption peak wavelengths tend to red-shift linearly with increasing NW radius. Also, one can see that sufficiently small NWs ($r < 15$ nm) can exhibit a very strong polarization dependence, i.e., Si NWs only support TM_{01} but no TE modes, whereas the polarization dependence for larger radii ($r > 80$ nm) exhibits such a different behavior that Q_{abs} tends to be higher for TE- than TM- polarized illumination. It is worth noting that the absorption cross section is bigger than the geometrical cross section, i.e., $Q_{abs} > 1$, indicating a strong absorption in Si NWs. For short $\lambda < {\sim}400$ nm, the absorption efficiency Q_{abs} shows a weak dependence on the radius r, attributed to the direct band gap nature of the Si with a high imaginary part of the complex refractive index. It is also worth noting that the calculated results for the polarized lights are qualitatively in good agreement with the recent report [11].
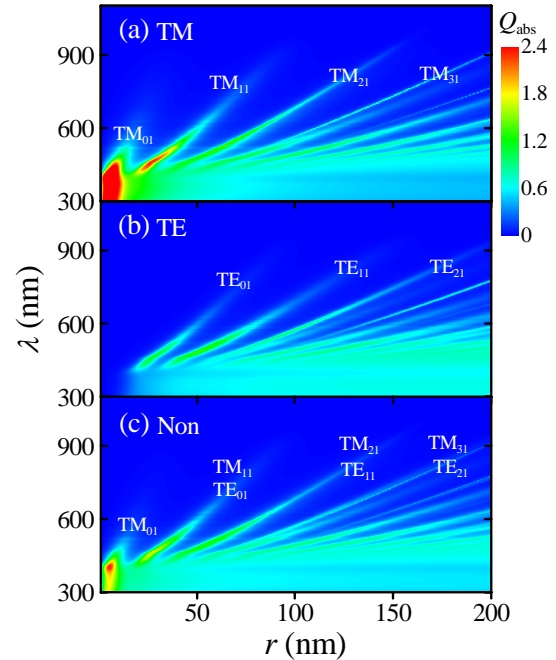
Fig. 2. Two-dimensional (2D) maps of the absorption efficiency Q_{abs} of Si NWs as a function of the wavelength λ and the radius r for (a) TM-polarized illumination, (b) TE - polarized illumination, and (c) Non - polarized illumination.

In addition, we present in Fig. 2(c) 2D color maps of Q_{abs} as a function of λ and r for non-polarized illumination. The calculations predict the locations of resonant absorption peaks, enabling their one-to-one correspondence to specific LMRs as TM_{01}, TM_{11}/ TE_{01}, TM_{21}/ TE_{11}, and TM_{31}/ TE_{21}. The results for the non-polarized illumination are also consistent with the recent reports [7, 11].

3.2 Single coaxial NWs

Considering the effect of the shell thickness t on the light absorption, we have calculated the absorption efficiency Q_{abs} in the coaxial NWs for the non-polarized illumination. In Fig. 3(a-d), we show the light absorption in the coaxial NWs of the shell refractive index $m_1 = 2.0$ as a function of the illumination wavelength λ and the shell thickness t for the core radius $r = 10, 50, 100,$ and 200 nm, respectively. As clearly seen from the figures, the absorption efficiency Q_{abs} is periodic in the shell thickness, showing the interference behavior of the Fano effect. Note that a thorough study of the Fano effect on coaxial NWs can be found in our recent work [9]. In the figures, the resonant peaks exhibit a red shift with increasing t at a given r (t-driven red-shift). As also seen from the figures, there are common characteristics between the coaxial NWs and Si NWs: The number of resonant peaks is augmented with increasing the core radius r, and these resonant peaks clearly tend to show a substantial red shift with increasing r (r-driven red-shift), consistent with our recent work [9].
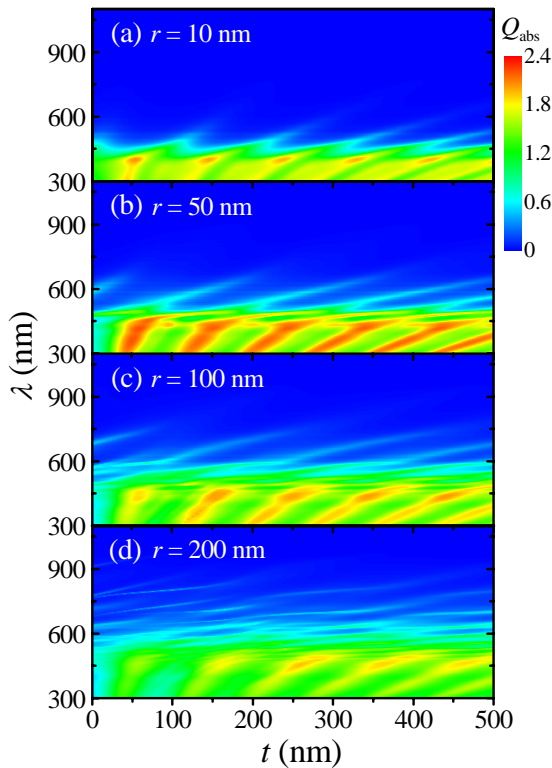
Fig. 3. 2D plots of the absorption efficiency Q_{abs} of coaxial NWs of the shell refractive index $m_1 = 2.0$ as a function of the wavelength λ and the shell thickness t for the core radius (a) $r = 10$ nm, (b) $r = 50$ nm, (c) $r = 100$ nm, and (d) $r = 200$ nm.

We next discuss the shell refractive index m_1 dependence of the light absorption in the coaxial NWs. In Fig. 4(a-d), we show the light absorption in the coaxial NWs of the shell thickness $t = 50$ nm as a function of the illumination wavelength λ and the shell refractive index m_1 for the core radius $r = 10, 50, 100,$ and 200 nm, respectively. It can be seen from the figures that the light absorption can be enhanced by tuning the shell refractive index m_1, especially for short $\lambda < \sim 600$ nm. When m_1 is very small, the absorption enhancement appears to be weak. As m_1 increases for a short λ, each light absorption at a given r reaches its resonance peak whose position depends on r. Similar to the effect of the shell thickness t on the light absorption above, the absorption efficiency has a periodic structure in the shell refractive index and the absorption peaks show a red shift with increasing m_1.
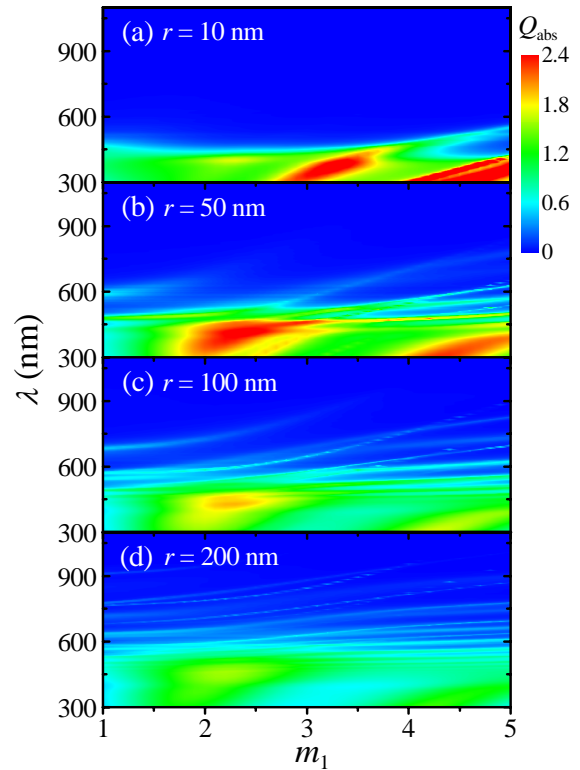
Fig. 4. 2D maps of the absorption efficiency Q_{abs} of coaxial NWs of the shell thickness $t = 50$ nm as a function of the wavelength λ and the shell refractive index m_1 for (a) $r = 10$ nm, (b) $r = 50$ nm, (c) $r = 100$ nm, and (d) $r = 200$ nm.

3.3 Photocurrent

Now, let us discuss a potential benefit of the coaxial NWs for PV applications. We have calculated the photocurrent density J_{sc} by integrating the product of Q_{abs}, elementary charge q, and the known AM 1.5G solar flux Γ as

$$J_{sc}\left(r,t\right) = q\int_{310\ nm}^{1127\ nm} Q_{abs}\left(\lambda,r,t\right)\Gamma\left(\lambda\right)d\lambda. \qquad (4)$$

In Fig. 5(a-d), we present 2D J_{sc} as a function of the shell thickness t and the shell refractive index m_1 for the core radius $r = 10, 50, 100,$ and 150 nm, respectively. As can be

seen in the figures, the photocurrent strongly depends on t, m_1, and r, showing that the photocurrent in single Si NWs can be further enhanced by coating the nonabsorbing dielectric shells.
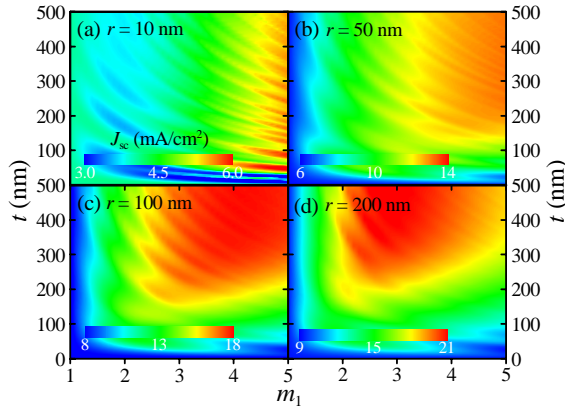
Fig. 5. 2D maps of the photocurrent density J_{sc} of coaxial NWs as a function of the shell thickness t and the shell refractive index m_1 for (a) r = 10 nm, (b) r = 50 nm, (c) r = 100 nm, and (d) r = 200 nm.
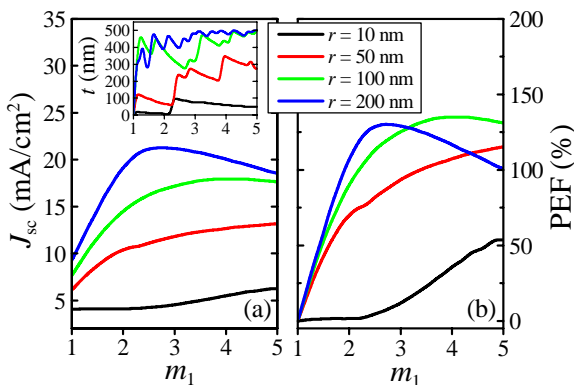
Fig. 6. (a) The photocurrent density J_{sc} of coaxial NWs versus the shell refractive index m_1. (b) The photocurrent enhancement factor (PEF) of coaxial NWs with respect to Si NWs versus the shell refractive index m_1. Inset: optimal the shell thickness t versus the shell refractive index m_1 for r = 10, 50, 100, and 200 nm.

Finally, we show in Fig. 6(a) the optimal J_{sc} as a function of the shell refractive index m_1. Note that the optimal J_{sc} corresponds to the optimal t in the inset of Fig. 6(a), yielded from Fig. 5. In Fig. 6(b), we show the photocurrent enhancement factor (PEF) of the coaxial NWs with respect to Si NWs as a function as m_1, calculated from Fig. 6(a). Here, the PEF is defined as $(J_{sc,cNW} - J_{sc,NW})/J_{sc,NW}$, where $J_{sc,cNW}$ and $J_{sc,NW}$ are the photocurrents for the coaxial NWs and Si NWs, respectively. The maximum J_{sc} (PEF) are 6.2 (54.0) ($t = 50$ nm, $m_1 = 4.9$), 13.1 (115.2) ($t = 50$ nm, $m_1 = 5$), 17.9 (135.0) ($t = 500$ nm, $m_1 = 4.2$), or 21.3 mA/cm^2 (130.2%) ($t = 445$ nm, $m_1 = 2.7$) for $r = 10, 50, 150,$ or 200 nm, respectively.

4. Conclusion

We have studied the light absorption in single coaxial NWs of Si cores and nonabsorbing dielectric shells for PV applications. We have demonstrated that the light absorption of the coaxial NWs can be significantly enhanced by tuning the core radius, the shell thickness, and the shell refractive index, leading to ~135% photocurrent enhancement as compared to Si NWs. Our results indicate that the coaxial NWs can be utilized for use in constructing high-efficiency NW PV devices.

References

[1] B. Tian, X. Zheng, T. J. Kempa, Y. Fang, N. Yu, G. Yu, J. Huang, C. M. Lieber, Nature **449**(7164), 885 (2007).
[2] A. I. Hochbaum, P. Yang, Chem. Rev. **110**(1), 527 (2010).
[3] K. Q. Peng, S. T. Lee, Adv. Mater. **23**(2), 198 (2011).
[4] C. Lin, M. L. Povinelli, Opt. Express **17**(22), 19371 (2009).
[5] H. Bao, X. Ruan, Opt. Lett. **35**(20), 3378 (2010).
[6] L. Cao, J. S. White, J. S. Park, J. A. Schuller, B. M. Clemens, M. L. Brongersma, Nat. Mater. **8**(8), 643 (2009).
[7] L. Cao, P. Fan, A. P. Vasudev, J. S. White, Z. Yu, W. Cai, J. A. Schuller, S. Fan, M. L. Brongersma, Nano Lett. **10**(2), 439 (2010).
[8] W. F. Liu, J. I. Oh, W. Z. Shen, Nanotechnology **22**(12), 125705 (2011).
[9] W. F. Liu, J. I. Oh, W. Z. Shen, IEEE Electron. Device Lett. **32**(1), 45 (2011).
[10] C. F. Bohren, D. R. Huffman, Absorption and Scattering of Light by Small Particles. (John Wiley & Sons, Inc., New York, 1998).
[11] G. Brönstrup, N. Jahr, C. Leiterer, A. Csáki, W. Fritzsche, S. Christiansen, ACS Nano **4**(12), 7113 (2010).
[12] David F. Edwards, "Silicon (Si)," in Handbook of Optical Constants of Solids, E. D. Palik, ed. (Academic, London, 1985).

_____
*Corresponding author: wfliu2301@163.com